

Inundation monitoring through high-resolution SAR/InSAR data and 2D hydraulic simulations

Alberto Refice¹, Guido Pasquariello¹, Annarita D'Addabbo¹, Fabio Bovenga¹, Raffaele Nutricato², Domenico Capolongo³, Annarita Lepera³, Luca Pietranera⁴, Salvatore Manfreda⁵, Andrea Cantisani⁵, Aurelia Sole⁵

¹ISSIA-CNR, Bari, Italy, e-mail refice@ba.issia.cnr.it

²GAP srl, c/o Dip. di Fisica "M. Merlin", Bari, Italy, e-mail raffaele.nutricato@gapslr.eu

³Earth e and Env. Science Dept., University of Bari, Italy, e-mail domenico.capolongo@uniba.it

⁴e-Geos s.p.a., Rome, Italy, e-mail luca.pietranera@e-geos.it

⁵School of Engineering, Univ. of Basilicata, Potenza, Italy, e-mail salvatore.manfreda@unibas.it

Abstract. In the present paper, COSMO-SkyMed high-resolution data acquired on the southern Basilicata region (Italy) are used for flood hazard monitoring. We concentrate on the flood event of Nov. 2-4, 2010, for which multi-temporal SAR data were available over the Bradano River downstream area in the same acquisition geometry, which allows interferometric processing. SAR intensity data analysis of two acquisitions dated 3 and 4 Nov., performed through optimized thresholding algorithms, shows good results, highlighting the temporal evolution of the flood throughout the two days, as also confirmed by a comparison with the results of a 2D hydraulic simulation of the same event. Additional use of the one-day co-event coherence channel, and then of more intensity and coherence data layers in the multi-temporal dataset, through automated clustering procedures, helps discriminating in more detail some uncertain cases regarding inundated fields, and suggest procedures to shed light on the spatio-temporal backscattering patterns of flood-prone areas.

Keywords. Flood monitoring, COSMO-SkyMed, InSAR coherence, 2D hydraulic modeling.

1. Introduction

The use of remotely sensed data for flood monitoring is a wide and complex field, which covers several research areas. A preliminary distinction can be made among emergency applications, which usually require fast processing and short-term availability of remotely sensed information to help in civil protection, search and rescue and first remediation operations, and damage assessment investigations, which can be performed on more relaxed time scales and involve off-line and more precise mapping procedures. Both types of activity greatly benefit from the availability of synthetic aperture radar (SAR) data, which are virtually insensitive to the adverse atmospheric conditions usually associated with flood events, in addition to being independent of sun illumination. The general working principle is based on the active nature of the sensor: radar backscatter level is negligible on calm water bodies, as compared to other non-flooded regions [1]. This simple behavior is influenced by the wealth of other factors affecting the actual backscattering level of the terrain, which include surface roughness and soil moisture, for land areas [2], and the presence of waves, for water bodies. These can locally modify the distribution of SAR backscatter values, hindering the identification of inundated areas. Other reasons for rogue variations in backscatter levels on flooded fields are given e.g. by the possible interaction of vegetation crops with the underlying water surface, resulting in double-bounce effects which strongly increase the backscatter. Occurrence of such conditions can be not so rare [3], especially in agricultural areas, where crops with rather stable vertical structure (e.g. wheat) and non-negligible radar penetration

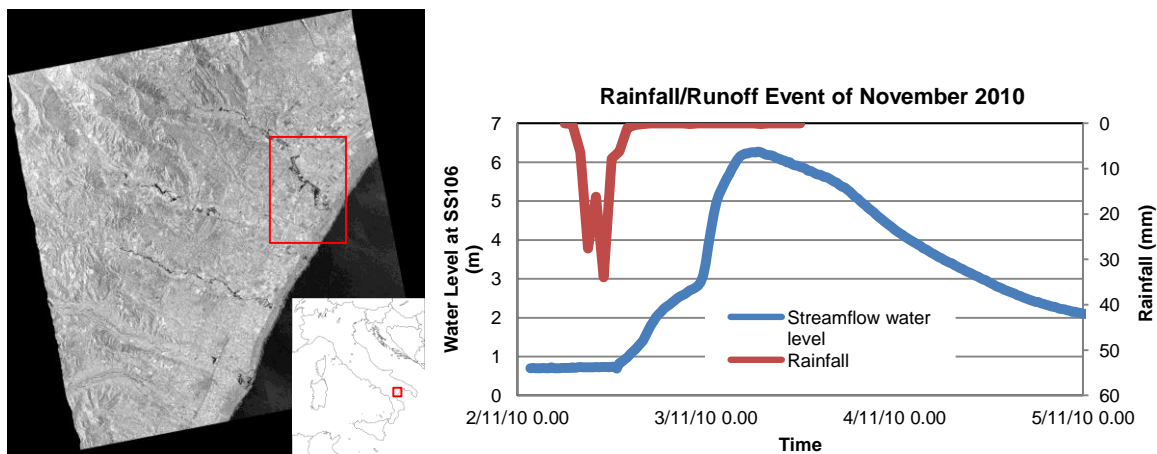


Figure 1. Left: location and overview (full-frame SAR intensity image) of the test site. Right: description of the flood event recorded during the November 2-4, 2010. The graph describes the temporal evolution of the water level recorded at the SS106 gauge station, and of the rainfall amount averaged over the basin area.

beneath the canopy are common. Recently, these problems have been tackled through radar backscatter modeling techniques, e.g. in [4].

An aid in resolving these issues may come from the availability of multi-temporal datasets, especially those allowing exploitation of the radar phase signal. Interferometric SAR (InSAR) coherence, in fact, carries information about the temporal stability of the microscopic arrangement of the individual scatterers concurring to the overall response of a SAR image cell [5]. Surfaces affected by flood retain changes leading to lower coherence values, with respect to unaffected areas. This effect is visible in a coherence image obtained by combining a pre- and a post-flood InSAR image pair, and carries information about the areas covered by water anytime during the interval between the acquisitions. Coherence computed from data by legacy sensors, such as those onboard the European ERS and ENVISAT satellites, have been successfully applied to flood monitoring [6],[7]. Obviously, then, InSAR is a very important piece of information to be used in synergy with other information layers, to improve the precision of flood maps from space.

Recently, interest in flood monitoring from space has received renewed attention due to the availability of latest-generation SAR sensors, such as the German TerraSAR-X and the Italian constellation COSMO-SkyMed. These instruments lead to improved monitoring capabilities, due to their high resolution and increased acquisition frequency, with repeat-pass intervals as short as a few hours in the case of emergency operation modes [3],[4].

We investigated flood events occurred in the Basilicata region, in Southern Italy, in the last three years, for which several COSMO-SkyMed acquisitions were available. In particular, in this work, we focus on one event occurred between 2 and 4 November, 2010. Various combinations of SAR and InSAR data, acquired over the area at times close to the event, were analyzed and processed through visual and automated classification algorithms to extract relevant information about flooded areas. Results were also compared with the inundation maps derived from 2-D hydraulic simulations aimed at the reproduction of the studied event [8].

2. Test site and dataset

Several basins in the Basilicata Region, Southern Italy, are subject, in recent times, to recurring flood events. The pressing importance of such phenomena becomes obvious in these semi-arid and sub-humid environments with long dry periods and short and intense rainfall episodes.

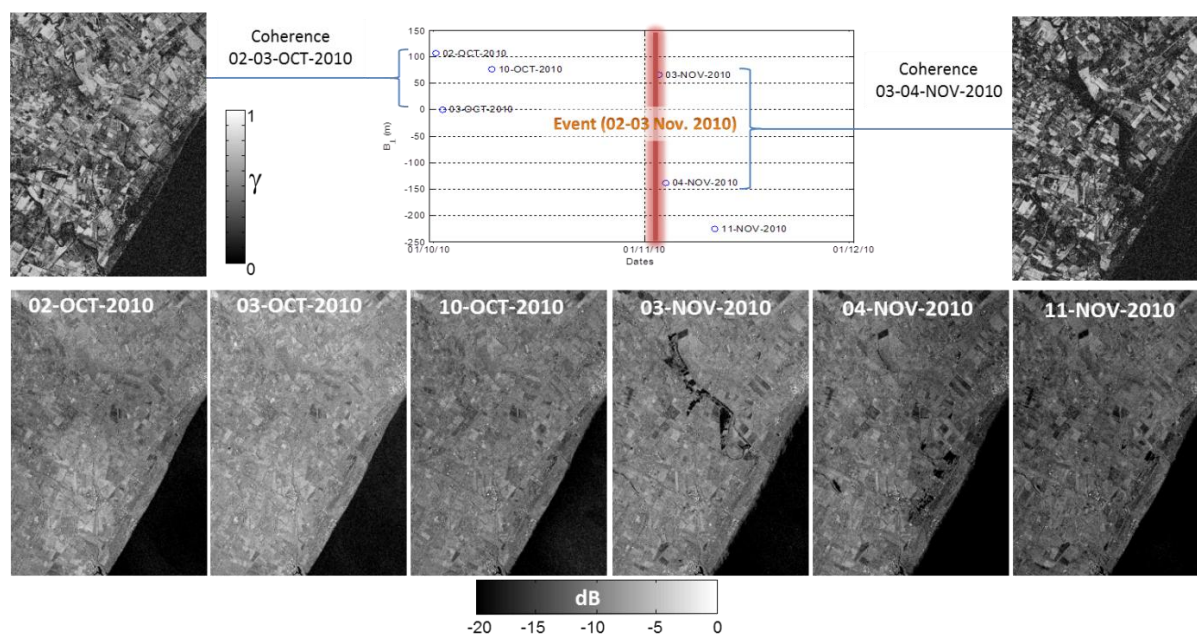


Figure 2. Center plot shows temporal and spatial baselines of the SAR images. The two one-day coherence images are shown on the top row, at the sides of the plot, for the area highlighted in red in **Figure 1**, while the six intensity images are shown at the bottom.

Such landscapes are affected by increased climate variability and climate-change related processes, leading to considerable socio-economic changes, as shown in several studies [e.g. 9]. Starting from the '50s, several water reservoirs for agricultural and industrial purposes have been constructed in the region. They are located along the principal rivers, Agri, Basento, Bradano, Cavone and Sinni, which flow into the Ionian Sea. The construction of the dams, associated to numerous hydraulic-forest works (bridges, reforestation), in addition to the important capture of sedimentary material from the river beds, have determined a drastic decrease of the solid transport, with consequent retreat of the Ionian shoreline. In addition, the agricultural land use of the alluvial plains has reduced the extent of the natural river bed, increasing flood risk. In the last five years, the frequency of extreme events has increased, causing several alluvial episodes, even two-three in the same year, with great damage for agriculture and industries. In particular, a recent study shows that the change in precipitation magnitude is due to multi-days, rather than single-day extreme precipitation events. The Bradano river basin is really emblematic for this sensitivity toward climate change and anthropogenic pressure. Due to its intrinsic lithological properties, in fact, the catchment, in its middle and final part, is mostly developed in Plio-pleistocene clays and Holocene sands [10], and it is prone to experience flash floods and widespread landsliding.

We focus on the inundation occurred on Nov. 2-4, 2010. The event was due to intense rainfall occurred in the late morning of November 2, which lasted about 6 hours, with most of it concentrated in two hours (10am-12am). A graphical representation of the time evolution of the event is given in the right panel of **Figure 1**, where we plot time series of the measured rainfall, as well as the water level measurements at the station SS106 located close to the outlet of the Bradano River. This River provoked inundations that affected several areas during the night between 2 and 3 Nov. 2010. The peak flow at the station SS106 was recorded on Nov. 3 at 6am. This peak produced an inundation that propagated in the surrounding areas, producing floods during November 3 and 4.

A total of 6 stripmap COSMO-SkyMed SAR images was available over the area (see left panel in **Figure 1** for location), with a ground pixel size of approximately $3 \times 3 \text{ m}^2$, acquired in the same geometry, polarization (VV), and incidence angle (38°), so that InSAR processing could be performed. The acquisition dates are 2, 3, and 10 October, 3, 4, and 11 November, 2010. As can be

seen, the two SAR acquisitions of 3 and 4 November offer a useful observation dataset to follow the temporal evolution of the flood wave phenomenon, while the other scenes may act as reference data.

Spatial and temporal baselines of the dataset are represented in the top-center plot of **Figure 2**, while in the bottom row of the same figure the six calibrated and geocoded intensity images of the area evidenced in the red rectangle in **Figure 1** are shown in logarithmic (dB) greyscale. It can be noticed how spatial baselines for the dataset are contained within a few hundred meters interval, which is an order of magnitude smaller than the critical baseline value for COSMO-SkyMed data. This ensures that geometric decorrelation is negligible, and so InSAR pairs exhibit coherence information which is mainly affected by temporal variations between the two acquisitions. Interferometric processing was thus performed through the DORIS open source software [11]. All the images were precisely co-registered using height information from SRTM data [12]. In the two side panels in **Figure 2**, the coherence images obtained from the two one-day interferometric pairs of 2-3 October (left) and 3-4 November (right), are shown in greyscale, with low (high) coherence corresponding to dark (bright) areas, respectively. Coherence was computed on a 11×11 pixels sliding window, previously removing the systematic topographic phase from the data.

3. Processing results

3.1. SAR intensity analysis

Water/non-water separation in single SAR images is usually accomplished by choosing a proper threshold value for the backscattering coefficient. Threshold values can be chosen in a variety of ways, both manually and automatically. Manual threshold tuning can be an operationally efficient methodology, indicated especially for emergency or time-critical applications, see e.g. [13]. SAR intensity analysis is usually preceded by filtering steps aimed at reducing the speckle noise on the images. This is especially useful as speckle noise may give rise to excessively fragmented final maps. We found that, in our case, an adequate amount of pre-filtering, operated on the input SAR intensity images, minimizes the need for post-processing operations such as majority filtering, which are often performed to limit the mentioned map fragmentation [4]. The SAR intensities were thus first fed to a Lee filter [14], with an iterated application, as specified in [15].

Automatically-derived thresholds can be set via a number of criteria [15]. Recently, an effective procedure has been proposed [16] for TerraSAR-X and applied [17] to COSMO-SkyMed data, based on the isolation of image windows characterized by a comparable population of “water” and “non-water” pixels, so that the local histograms exhibits a sufficiently bi-modal character to properly set the threshold value. This is usually set through the so-called Kittler-Illingworth (KI) criterion [18]. Application of this methodology to our data gives interesting results, some of which are shown in **Figure 3**. As can be seen, the two images of 3-4 Nov. clearly show different inundated areas, highlighting the downstream temporal evolution of the phenomenon (panels A-B).

The consistence of this multi-temporal SAR intensity analysis was tested using for comparison the result of the hydraulic model Flora-2D (FLOOD and Roughness Analysis) [19]. This model is a product of a collaboration between the School of Engineering of the University of Basilicata and the company “Research on energy System (RSE). The general algorithm governing the flood propagation is based on the “shallow water equations” simplified by eliminating the convective terms [20]. Modeling was carried out by using a LiDAR-derived digital elevation model (DEM) with 5 m of resolution and roughness coefficients defined on the land-use map of the area. The model provides hourly simulated maps of surface water depth in each pixel of the modeled domain. Two such maps were generated for the exact acquisition times of the two SAR scenes. These, shown in **Figure 4**, highlight a general agreement with the SAR data monitoring of the flood

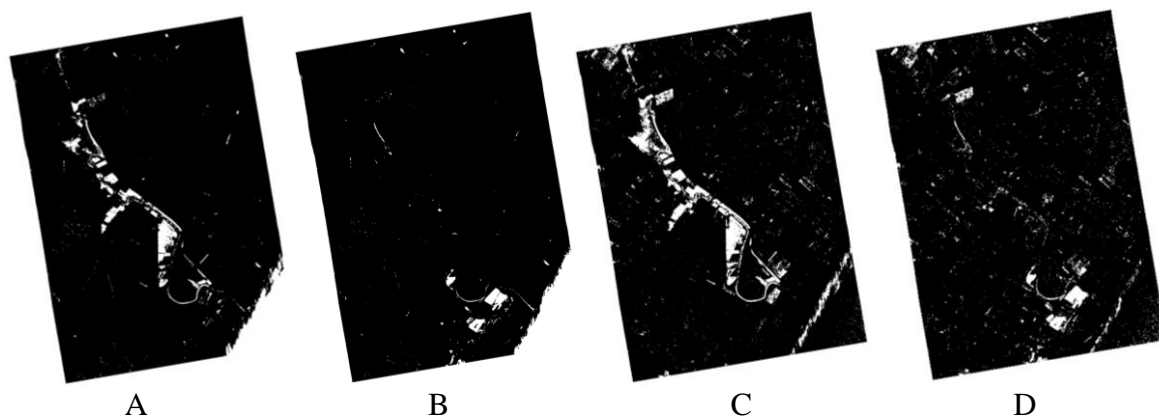


Figure 3. Results of intensity thresholding based on the split-based algorithm mentioned in the text. A-B: binary flood maps obtained by split-based intensity thresholding for the dates of Nov. 3 and 4, 2010, respectively; C-D: binary maps obtained by split-based thresholding change maps of, resp., 3 and 4 Nov., with respect to the same reference map of 10 Oct.

evolution, showing different patterns of inundated areas on the two dates. Nevertheless, on a more local scale, there are differences between the flood areas detected on the SAR images and those predicted by the model. Some improvement can be gained by using additional information, for instance analyzing the differences in intensity between images acquired during the event and pre-flood images. Two such maps, obtained by thresholding, through the same optimized procedure, the differences of the 3 and 4 Nov. images, respectively, with the 10 Oct. reference image, are shown in **Figure 3-C-D**. The detected flooded areas appear more extended and homogeneous in this case than in the single-date threshold maps (A-B), and, overall, the agreement with the hydraulic modeling seems to improve. Some discrepancies, however, remain. The causes of such discrepancies are currently under investigation.

3.2. Coherence analysis

An effective way of visually combining information from intensity and coherence images of an InSAR pair is to assign each image, or combinations thereof, to the channels of an RGB image. For example, in **Figure 5**, an RGB combination of the two SAR intensity and the coherence for the 3-4 Nov. 2010 pair is shown, for the same area highlighted in red in the map on the left in **Figure 1**. It is possible to recognize areas flooded only on 3 Nov., characterized by greenish colors, as well as other areas flooded only on 4 Nov., characterized by reddish colors. Two fields are evidenced by ellipses: these are fields which are classified as “water” in both the single-date, and the change intensity-based flood maps (see **Figure 3**), while their relatively high coherence value (blue color) suggests they were likely not interested by the flood in neither date. Indeed, in situ investigations allowed to ascertain that the two fields are actually standing some tenths of meter above the ground level of neighboring fields, which supports the hypothesis that they were not flooded during the event, as was finally confirmed by interviews with local farmers.

3.3. Joint multi-source data clustering

Besides the examples highlighted in the preceding sections, use of SAR multi-temporal information, both as intensity and phase data, presents a quantity of additional information for the analysis of areas subject to floods. We then use an unsupervised clustering approach to attempt to organize and interpret this information. The approach is based on the well-known K-means algorithm, which works grouping data in K disjoint clusters, where K is fixed in advance [21]. Our implementation of K-means starts by selecting at random K input data as representative vectors, and

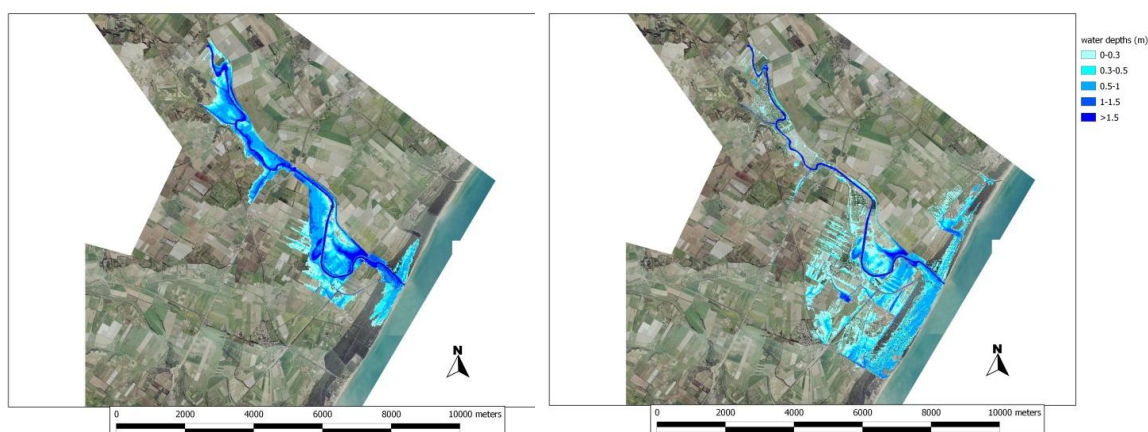


Figure 4. Flood maps obtained from the Flora2D model for the 3 (left) and 4 (right) Nov., 2010, at the time of the COSMO/SkyMed acquisitions.

then assigning each image pixel to the cluster having the closest centroid. When all data have been assigned, the positions of the K centroids are recomputed. This procedure is repeated until there is no further change in the grouping of data points and the algorithm converges. We use this simplified approach, which considers each image pixel as independent from all the others, relying on the spatial homogeneity ensured by the pre-processing, as shown in the preceding sections.

Several tests were performed by varying both the K value and the number and type of input data layers. In **Figure 6** we show a map highlighting only the most meaningful 3 clusters resulting from an experiment using as input the two intensity (3 and 4 Nov.) and the two coherence (2-3 Oct., 3-4 Nov.) layers, with a total number $K = 16$ of output clusters. The two temporally separated areas, flooded on 3 and 4 Nov, respectively, appear classified in two different clusters, while the third considered cluster contains the fields identified as “false alarms” in the preceding sections, as well as other fields not investigated in situ. The two plots on the right show the average cluster centroid layer values for the three classes. Also, the values computed on the two single fields, indicated by the letters “A” and “B” in **Figure 5** and described in the preceding section, are shown on the plot.

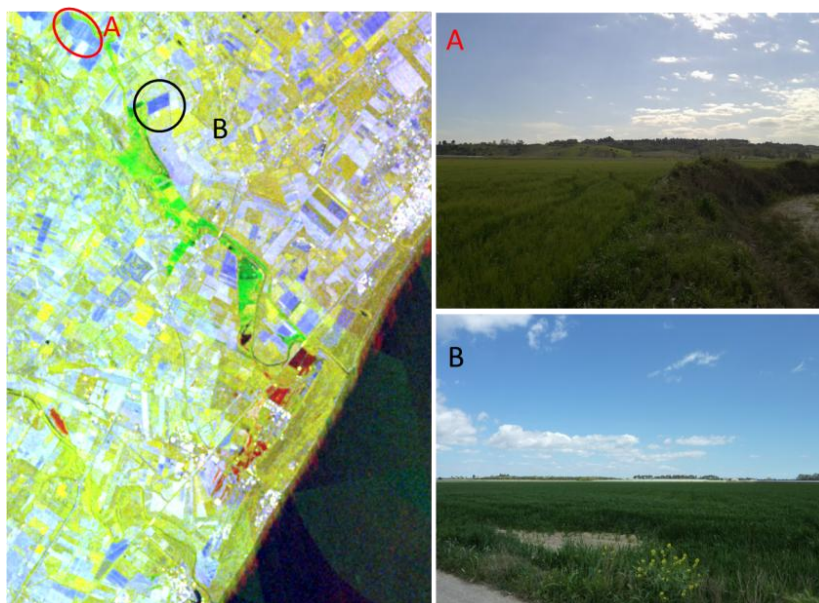


Figure 5. Left: RGB composite of 2 intensity images and one coherence image (R = Nov. 3 intensity, G = Nov. 4 intensity, B = 3-4 Nov. InSAR coherence). The “A” and “B” highlighted fields containing “false alarms” are evidenced, with pictures, taken in situ, shown on the right.

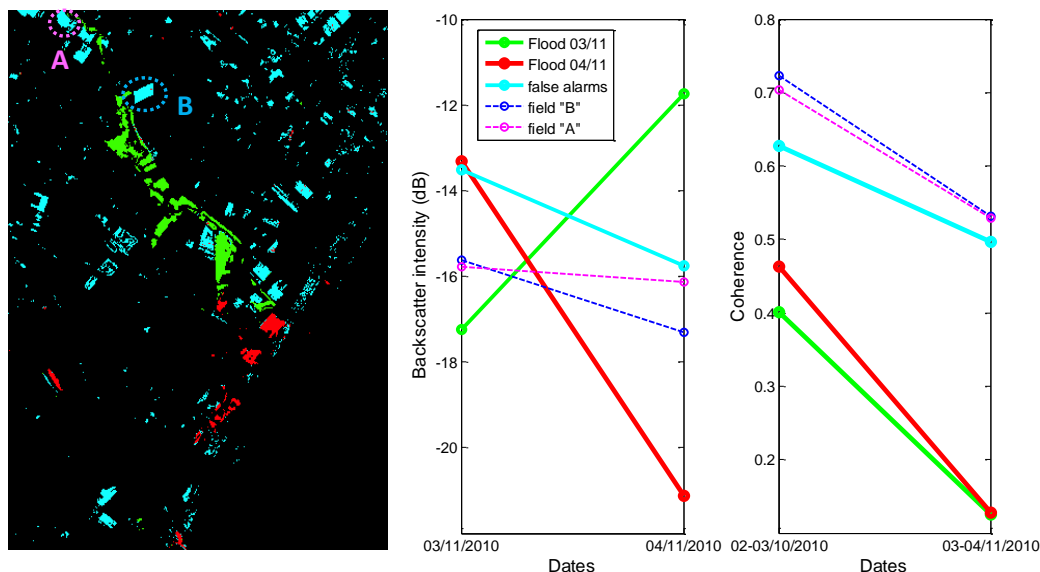


Figure 6. Results of the clustering of two intensity (3 and 4 Nov) and two coherence (2-3 Oct. and 3-4 Nov.) maps. Left: map with 3 highlighted clusters (out of the total of 16). Right: trends of the 2 intensity and the 2 coherence bands for the three selected clusters, as well as those computed on the fields “A” and “B” indicated by the dashed ellipses (see also left panel in Figure 5).

As can be seen, intensity information alone (left plot) could lead to misclassify those fields as “water”, due to their rather low intensity, while their high values in the coherence channels allow to correctly identify them as false alarms.

Ongoing experiments on other similar cases highlight the increasing discrimination capability of statistically-based clustering algorithms as more information, coming from multi-temporal data, is added to the input dataset. This also helps towards the aim of comparing and interpreting the results with respect to those obtained by the hydraulic modeling.

4. Conclusions

Analysis of a multi-temporal dataset of COSMO-SkyMed stripmap data was carried out over a test site in the Basilicata region (Southern Italy), affected by a flood event occurred in the first days of Nov., 2010. Automated, split-based thresholding of single-date intensity images acquired on 3 and 4 Nov., give flood maps which allow to follow separately the two-day evolution of the event. Use of additional pre-flood intensity information increases the reliability of the results, which exhibit interesting similarities with water depth maps obtained through 2-D hydraulic simulation of the event at the times of the two satellite overpasses.

Use of InSAR coherence information improves the detection of false alarms, such as fields covered by vegetation and not affected by the flood, and increases the possibility of gaining insight into multi-temporal land-cover changes. Multi-layer information can be analyzed systematically through unsupervised clustering techniques, confirming the increased usefulness of multi-temporal SAR data analysis to understand, and physically and hydraulically model, changes in surfaces due to flood events.

Acknowledgements

COSMO-SkyMed data were courtesy of e-Geos s.p.a. The authors thank Dr. Ing. D. O. Nitti, of Geophysical Application Processing s.r.l., for the InSAR data processing.

References

- [1] Weydahl, D J, 1996. *Flood monitoring in Norway using ERS-1 SAR images*. 1996 International Geoscience and Remote Sensing Symposium vol 1 (IEEE) pp 151–3
- [2] Mattia, F., Satalino G, Dente L and Pasquariello G, 2006. *Using a priori information to improve soil moisture retrieval from ENVISAT ASAR AP data in semiarid regions*. IEEE Transactions on Geoscience and Remote Sensing, **44** 900–12
- [3] Pierdicca, N., Pulvirenti, L., Chini, M., Guerriero, L. and Candela, L., 2013. *Observing floods from space: Experience gained from COSMO-SkyMed observations*. Acta Astronautica, **84** 122–33
- [4] Pulvirenti, L., Chini, M., Pierdicca, N., Guerriero, L. and Ferrazzoli, P., 2011. *Flood monitoring using multi-temporal COSMO-SkyMed data: Image segmentation and signature interpretation*. Remote Sensing of Environment, **115** 990–1002
- [5] Geudtner, D., Winter, R. and Vachon, P. W., 1996. *Flood monitoring using ERS-1 SAR interferometry coherence maps*. IGARSS '96. 1996 International Geoscience and Remote Sensing Symposium vol 2 (IEEE) pp 966–8
- [6] Nico, G., Pappalepore, M., Pasquariello, G., Refice, A. and Samarelli, S., 2000. *Comparison of SAR amplitude vs. coherence flood detection methods - a GIS application*. International Journal of Remote Sensing, **21** 1619–31
- [7] Dellepiane, S., Bo, G., Monni, S. and Buck, C., 2000. *SAR images and interferometric coherence for flood monitoring*. International Geoscience and Remote Sensing Symposium 2000 vol 6 (IEEE) pp 2608–10
- [8] Manfreda, S., Di Leo, M. and Sole, A., 2011. *Detection of Flood-Prone Areas Using Digital Elevation Models*. Journal of Hydrologic Engineering, **16** 781–90
- [9] Piccarreta, M., Capolongo, D., Boenzi, F. and Bentivenga, M., 2006. *Implications of decadal changes in precipitation and land use policy to soil erosion in Basilicata, Italy*. CATENA, **65** 138–51
- [10] Boenzi, F., Caldara, M., Capolongo, D., Dellino, P., Piccarreta, M. and Simone, O., 2008. *Late Pleistocene–Holocene landscape evolution in Fossa Bradanica, Basilicata (southern Italy)*. Geomorphology, **102** 297–306
- [11] Kampes, B., Hanssen, R. and Perski, Z., 2003. *Radar interferometry with public domain tools*. Proceedings of FRINGE,
- [12] Nitti, D. O., Hanssen, R. F., Refice, A., Bovenga, F. and Nutricato, R., 2011. *Impact of DEM-Assisted Coregistration on High-Resolution SAR Interferometry*. IEEE Transactions on Geoscience and Remote Sensing, **49** 1127–43
- [13] Boni, G., Candela, L., Castelli, F., Dellepiane, S., Palandri, M., Persi, D., Pierdicca, N., Rudari, R., Serpico, S., Siccardi, F. and Versace, C., 2009. *The OPERA project: EO-based flood risk management in Italy*. 2009 IEEE International Geoscience and Remote Sensing Symposium (IEEE) pp II–929–II–932
- [14] Lee, J.-S., 1986. *Speckle Suppression And Analysis For Synthetic Aperture Radar Images*. Optical Engineering, **25** 255636
- [15] Bazi, Y., Bruzzone, L. and Melgani, F., 2005. *An unsupervised approach based on the generalized Gaussian model to automatic change detection in multitemporal SAR images*. IEEE Transactions on Geoscience and Remote Sensing, **43** 874–87
- [16] Martinis, S., Twele, A. and Voigt, S., 2009. *Towards operational near real-time flood detection using a split-based automatic thresholding procedure on high resolution TerraSAR-X data*. Natural Hazards and Earth System Science, **9** 303–14
- [17] Bellifemine, V., Bovenga, F., Candela, L., Nutricato, R., Pasquariello, G. and Refice, A., 2010. *Identificazione di aree inondate da immagini SAR a media ed alta risoluzione*. ASITA 2010 vol 610 pp 211–6
- [18] Kittler, J. and Illingworth, J., 1986. *Minimum error thresholding*. Pattern Recognition, **19** 41–7
- [19] Cantisani, A., 2012. *Monitoraggio e modellazione per la protezione dal rischio idraulico in aree pianeggianti mediante lo sviluppo e l'applicazione di modelli bidimensionali e l'utilizzo di strumenti GIS Open Source (Università della Basilicata)*
- [20] Molinaro, P., Fillippo, A., Di Ferrari, F. and Di Filippo, A., 1994. *Modelling of flood wave propagation over flat dry areas of complex topography in presence of different infrastructures*. Modelling of Flood Propagation Over Initially Dry Areas, **1** 209–28
- [21] Bishop, C., 1995. *Neural networks for pattern recognition* vol 92 (Oxford University Press, USA)